

Anisotropic magnetic order of the Eu sublattice in single crystals of $\text{EuFe}_{2-x}\text{Co}_x\text{As}_2$ ($x = 0, 0.2$) studied by means of magnetization and magnetic torque

Z. Guguchia,* S. Bosma, and S. Weyeneth

Physik-Institut der Universität Zürich, Winterthurerstrasse 190, CH-8057 Zürich, Switzerland

A. Shengelaya

Department of Physics, Tbilisi State University, Chavchavadze 3, GE-0128 Tbilisi, Georgia

R. Puzniak

Institute of Physics, Polish Academy of Sciences, Aleja Lotników 32/46, PL-02-668 Warsaw, Poland

Z. Bukowski† and J. Karpinski

Laboratory for Solid State Physics, ETH Zürich, CH-8093 Zürich, Switzerland

H. Keller

Physik-Institut der Universität Zürich, Winterthurerstrasse 190, CH-8057 Zürich, Switzerland

(Received 11 July 2011; published 4 October 2011)

We present a combination of magnetization and magnetic torque experiments to investigate the magnetic orders in undoped EuFe_2As_2 and Co-doped $\text{EuFe}_{1.8}\text{Co}_{0.2}\text{As}_2$ single crystals. Although at low temperatures typical results for an antiferromagnetic (AFM) state in EuFe_2As_2 were found, our data strongly indicate the occurrence of a canted antiferromagnetic (C-AFM) order of the Eu^{2+} moments between 17 and 19 K, observed even in the lowest studied magnetic fields. However, unlike in the parent compound, no low-field and low-temperature AFM state of the Eu^{2+} moments was observed in the doped $\text{EuFe}_{1.8}\text{Co}_{0.2}\text{As}_2$. Only a C-AFM phase is present at low fields and low temperatures, with a reduced magnetic anisotropy as compared to the undoped system. We discuss for both EuFe_2As_2 and $\text{EuFe}_{1.8}\text{Co}_{0.2}\text{As}_2$ the experimentally deduced magnetic phase diagrams of the magnetic ordering of the Eu^{2+} sublattice with respect to the temperature, the applied magnetic field, and its orientation to the crystallographic axes. It is likely that the magnetic coupling of the Eu and the Fe sublattice is strongly dependent on Co doping, having detrimental influence on the magnetic phase diagrams as determined in this work. Their impact on the occurrence of superconductivity with higher Co doping is discussed.

DOI: [10.1103/PhysRevB.84.144506](https://doi.org/10.1103/PhysRevB.84.144506)

PACS number(s): 74.70.Xa, 75.30.Gw, 75.30.Kz, 75.50.Ee

I. INTRODUCTION

The discovery of superconductivity in the iron-based pnictides¹ provided a new class of compounds to the high-temperature-superconductor (HTS) family. Three main groups of these iron-based superconductors are intensively studied: the $R\text{FeAsO}$ compounds with $R = \text{La-Gd}$ (1111),^{1,2} the ternary arsenides $A\text{Fe}_2\text{As}_2$ with $A = \text{Ba, Sr, Ca, Eu}$ (122),³ and the binary chalcogenides such as FeSe_{1-x} (11).⁴ Similar to the cuprate HTS's, the undoped iron pnictides are not superconducting (SC) at ambient pressure and undergo a spin-density wave (SDW) transition at high temperatures.⁵ The SC state in iron-based compounds can be achieved either under pressure (chemical and hydrostatic)⁶⁻¹⁵ or by appropriate charge-carrier doping of the parent compounds,¹⁶⁻¹⁸ both accompanied by a suppression of the SDW state.

Here, we focus on EuFe_2As_2 , which is a particularly interesting member of the ternary system $A\text{Fe}_2\text{As}_2$, since the A site is occupied by a rare-earth Eu^{2+} S -state (orbital moment $L = 0$) ion with a $4f^7$ electronic configuration. Eu^{2+} has a total electron spin $S = 7/2$, corresponding to a theoretical effective magnetic moment of $7.94 \mu_B$. It is the only known member of the 122 family containing $4f$ electrons. In addition to the SDW ordering of the Fe moments at $T_{\text{SDW}} \simeq 190$ K, an antiferromagnetic (AFM) order of the Eu^{2+} spins at $T_{\text{AFM}} \simeq 19$ K was reported by Mössbauer

and susceptibility measurements.¹⁹⁻²¹ Recently, neutron diffraction measurements were performed on EuFe_2As_2 and the magnetic structure illustrated in Fig. 1 was established.⁵ This material exhibits an A -type AFM order of the Eu^{2+} moments, e.g., the Eu^{2+} spins align ferromagnetically in the planes, while the planes are coupled antiferromagnetically.^{5,22} It was demonstrated that, by applying a high enough magnetic field, the Eu^{2+} moments can be realigned ferromagnetically in both the parent compound EuFe_2As_2 (Refs. 21 and 23) as well as in the Co-doped system $\text{EuFe}_{2-x}\text{Co}_x\text{As}_2$ ($x = 0.22$).²⁴ In addition, neutron diffraction measurements²³ suggested a canted AFM (C-AFM) structure of the Eu^{2+} moments in EuFe_2As_2 at intermediate magnetic fields.

Co-substitution induces superconductivity in $\text{EuFe}_{2-x}\text{Co}_x\text{As}_2$ with a reentrant behavior of resistivity due to the AFM ordering of the Eu^{2+} spins.²⁵ Reentrant superconducting behavior was also observed in resistivity experiments on EuFe_2As_2 under an applied pressure up to 2.5 GPa.^{14,15} However, only above 2.8 GPa, where a valence change of the Eu ions from a divalent magnetic state ($4f^7$, $J = 7/2$) to a trivalent nonmagnetic state ($4f^6$, $J = 0$) was suggested to occur,⁷ a sharp transition to a zero-resistivity state was observed.¹⁴ Bulk superconductivity was also achieved in $\text{EuFe}_2\text{As}_{2-x}\text{P}_x$,^{7,26} where isovalent P substitution of the As site induces chemical pressure in EuFe_2As_2 . No

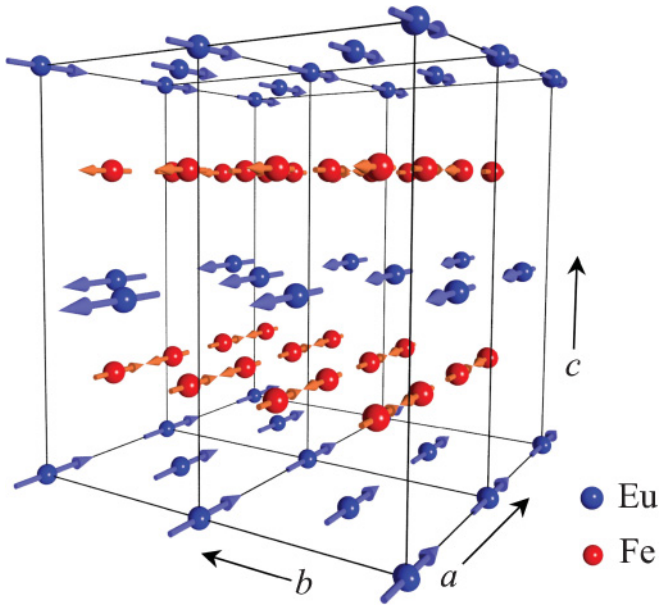


FIG. 1. (Color online) Schematic illustration of the magnetic structure of EuFe_2As_2 . The Fe moments (red) form a SDW state, whereas the Eu moments (blue) order ferromagnetically in the ab plane and align antiferromagnetically along the c axis.

superconductivity was detected in $\text{EuFe}_{2-x}\text{Ni}_x\text{As}_2$,²⁷ while superconductivity with a maximum $T_c \simeq 20$ K was reported for $\text{BaFe}_{2-x}\text{Ni}_x\text{As}_2$.²⁸ It was suggested in various reports^{21,27,29,30} that there is a strong coupling between the localized Eu^{2+} spins and the conduction electrons of the Fe_2As_2 layers. Recently, the hyperfine coupling constant A_{Eu} between the ^{75}As nuclei and the Eu $4f$ states in $\text{EuFe}_{1.9}\text{Co}_{0.1}\text{As}_2$ was quantitatively determined from ^{75}As nuclear magnetic resonance (NMR) to be $A_{\text{Eu}} = -1.9 \times 10^7$ A/m μ_B .³¹ This large value of A_{Eu} indicates a strong coupling between the Eu^{2+} localized moments and the charge carriers in the Fe_2As_2 layers, and points to a strong correlation between the ordering of the localized magnetic moments and superconductivity in $\text{EuFe}_{2-x}\text{Co}_x\text{As}_2$.

It is well established that the SDW state of the Fe moments is suppressed as a result of Co doping. However, at present, there is no clear picture as to how the ordering of the Eu spins develops with increasing Co concentration. Generally, it was assumed that, in the 122 systems, the direction of the sublattice magnetization of the Eu^{2+} magnetic moments is strongly affected by the magnetic behavior of the Fe atoms.^{5,32–36} Thus, it is important to compare the magnetic properties of the Eu sublattice in $\text{EuFe}_{2-x}\text{Co}_x\text{As}_2$ without and with Co doping in order to study the correlation between ordering of Eu^{2+} moments and the magnetism of the Fe sublattice. This, in turn, is crucial to understand the interplay between magnetism of localized moments and superconductivity in $\text{EuFe}_{2-x}\text{Co}_x\text{As}_2$.

In this paper, we present magnetic susceptibility, magnetization, and magnetic torque experiments performed on single crystals of $\text{EuFe}_{2-x}\text{Co}_x\text{As}_2$ ($x = 0, 0.2$). The goal of this study is to investigate the macroscopic magnetic properties of the Eu sublattice. Magnetic susceptibility and magnetization investigations provide information on the magnetic structure of a single-crystal sample in magnetic fields applied along the principal axes. In addition, the evolution of the magnetic

structure as a function of the tilting angle of the magnetic field and the crystallographic axis can be studied by magnetic torque. This paper is organized as follows: Experimental details are described in Sec. II. The results of the magnetic susceptibility, the magnetization, and the magnetic torque measurements are presented and discussed in Sec. III. In Sec. IV, the magnetic phase diagrams of the Eu^{2+} sublattice ordering with respect to magnetic field and temperature in single crystals of $\text{EuFe}_{2-x}\text{Co}_x\text{As}_2$ ($x = 0, 0.2$) are discussed. The conclusions follow in Sec. V.

II. EXPERIMENTAL DETAILS

Single crystals of $\text{EuFe}_{2-x}\text{Co}_x\text{As}_2$ ($x = 0, 0.2$) were grown out of Sn flux.³¹ The magnetization measurements of the $\text{EuFe}_{2-x}\text{Co}_x\text{As}_2$ ($x = 0, 0.2$) samples were performed with a commercial SQUID magnetometer (*Quantum Design* MPMS-XL) with the magnetic field H applied parallel ($H \parallel c$) or perpendicular ($H \perp c$) to the crystallographic c axis. The magnetic torque measurements were carried out using a homemade torque sensor.³⁷ The sample is mounted on a platform hanging on piezoresistive legs. A magnetic field \vec{H} applied to the sample having magnetic moment \vec{m} results in a mechanical torque $\vec{\tau} = \mu_0 \vec{m} \times \vec{H}$. This torque bends the legs, and thus creates a measurable electric signal proportional to the torque amplitude. The temperature is controlled by an *Oxford* flow cryostat, and the magnetic field is provided by a rotatable resistive *Bruker* magnet with a maximum magnetic field of 1.4 T.

III. RESULTS

A. Magnetization measurements

1. Temperature dependence

The temperature dependence of the magnetic susceptibility $\chi = M/H$ (here M is the magnetization determined as magnetic moment per mol) for the crystal of EuFe_2As_2 in a field of $\mu_0 H = 0.01$ T for $H \perp c$ and for $H \parallel c$ is shown in Fig. 2(a). In agreement with previous reports,^{20,21} the magnetic susceptibility for $H \perp c$ (χ_{\perp}) and for $H \parallel c$ (χ_{\parallel}), determined in the temperature range from 30 to 190 K (i.e., far above $T_{\text{AFM}} \simeq 19$ K of the Eu moments up to $T_{\text{SDW}} \simeq 190$ K of the Fe moments) is well described by the Curie-Weiss law

$$\chi(T) = \frac{C}{T - \theta_{\text{CW}}}. \quad (1)$$

Here, C denotes the Curie constant and θ_{CW} the Curie-Weiss temperature. Analyzing the data in Fig. 2(a) with Eq. (1) yields $C = 1853(15) \times 10^{-7}$ m³ K/mol, $\theta_{\text{CW}} = 19.74(8)$ K for $H \parallel c$ and $C = 2127(23) \times 10^{-7}$ m³ K/mol, $\theta_{\text{CW}} = 20.69(4)$ K for $H \perp c$. The calculated effective magnetic moment is $\mu_{\text{eff}} \simeq 7.6 \mu_B$ for $H \parallel c$ and $\mu_{\text{eff}} \simeq 8.3 \mu_B$ for $H \perp c$. These estimates of μ_{eff} are close to the theoretical value of the magnetic moment of a free Eu^{2+} ion ($\mu_{\text{Eu}^{2+}} = 7.94 \mu_B$). The positive value of θ_{CW} for both $H \parallel c$ and $H \perp c$ is consistent with previous magnetization measurements,^{20,21} indicating that the direct interaction between the Eu^{2+} moments is ferromagnetic (FM). This is in agreement with the magnetic structure of EuFe_2As_2 suggested by zero-field neutron diffraction measurements,⁵

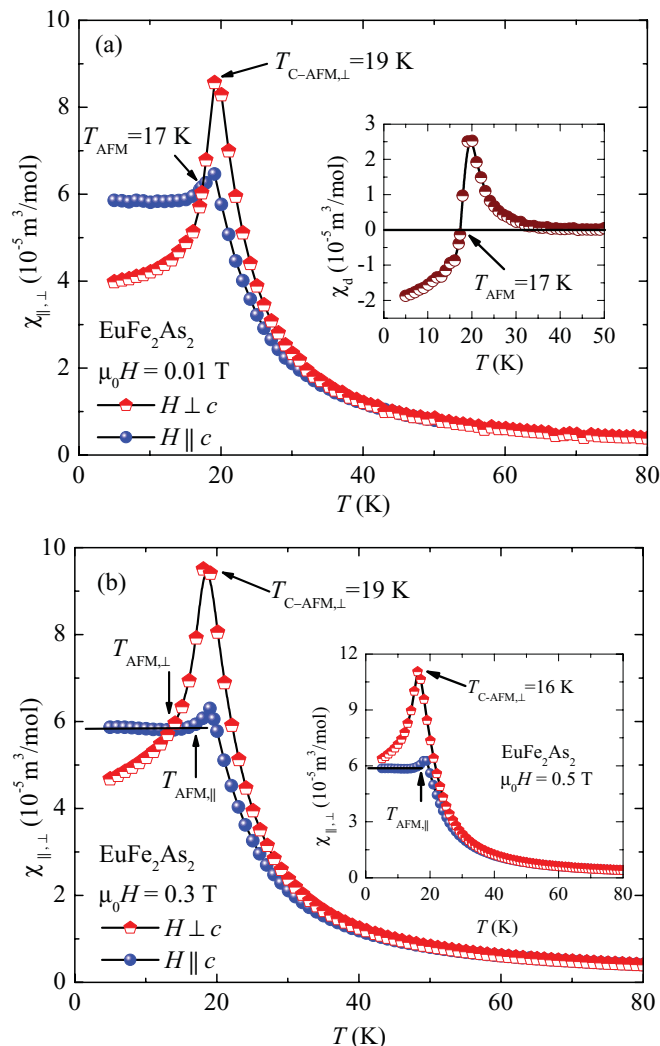


FIG. 2. (Color online) Temperature dependence of the magnetic susceptibility measured at fixed magnetic fields applied perpendicular ($H \perp c$) and parallel ($H \parallel c$) to the crystallographic c axis of single-crystal EuFe_2As_2 : (a) $\mu_0 H = 0.01$ T; (b) $\mu_0 H = 0.3$ T and $\mu_0 H = 0.5$ T (inset). The inset of panel (a) illustrates the temperature dependence of the difference between both susceptibilities ($\chi_d = \chi_{\perp} - \chi_{\parallel}$). The arrows mark the AFM and C-AFM ordering temperatures of the Eu^{2+} moments, and $T_{\text{AFM},\perp}$ and $T_{\text{AFM},\parallel}$ refer to the AFM ordering temperatures for $H \perp c$ and $H \parallel c$, respectively. The canted-AFM ordering temperature for $H \perp c$ is denoted by $T_{\text{C-AFM},\perp}$.

revealing that the intralayer arrangement of the Eu^{2+} spins is FM. The sharp increase of χ with decreasing temperature below 30 K also indicates a FM coupling between the Eu^{2+} moments. The Eu moments align with respect to the Fe moments along the a axis⁵ as illustrated in Fig. 1.

With decreasing temperature from 19 to 17 K, the susceptibility χ_{\perp} of single-crystal EuFe_2As_2 decreases rapidly, and below 17 K, the decrease of χ_{\perp} is less pronounced. On the other hand, χ_{\parallel} decreases with decreasing temperature from 19 to 17 K and remains constant below 17 K. Moreover, the values of χ_{\perp} and χ_{\parallel} at 19 K are substantially different ($\chi_{\perp}/\chi_{\parallel} \simeq 1.33$), already in a rather low magnetic field $\mu_0 H = 0.01$ T [see Fig. 2(a)]. Note that within the classical picture

of an ideal antiferromagnet, the magnetic susceptibility χ in a magnetic field perpendicular to the easy axis is constant, and χ in a field parallel to the easy plane decreases linearly with decreasing temperature. In addition, for an antiferromagnet, the values of χ at the antiferromagnetic (AFM) transition temperature are the same for both $H \perp c$ and $H \parallel c$.²² The inset of Fig. 2(a) illustrates the temperature dependence of the difference between both susceptibilities $\chi_d = \chi_{\perp} - \chi_{\parallel}$. Note that, below 19 K, the quantity χ_d decreases with decreasing temperature and reaches zero at around 17 K. This behavior of $\chi_d(T)$ can be explained by invoking a transition from the high-temperature paramagnetic state to a FM state or to a C-AFM state at about 19 K. The transition from a FM or a C-AFM to an AFM state of the Eu^{2+} spins occurs only below 17 K. The pronounced increase of χ_{\parallel} above 17 K indicates the appearance of a magnetic moment along the c axis. Since χ_{\parallel} is smaller than χ_{\perp} in the FM/C-AFM state, it is suggested that the ab plane is the easy plane of this ordered state. In Fig. 2(b), the temperature dependences of χ_{\perp} and χ_{\parallel} of single-crystal EuFe_2As_2 in a magnetic field of 0.3 and 0.5 T (inset) are shown. Obviously, the AFM transition temperatures for $H \perp c$ (crossing point of χ_{\perp} and χ_{\parallel}) and for $H \parallel c$ (temperature at which χ_{\parallel} starts to increase) are shifted to lower temperature with higher magnetic field [see Fig. 2(a) for comparison]. However, at $\mu_0 H = 0.5$ T, the curves χ_{\perp} and χ_{\parallel} do not cross in the investigated temperature range, indicating that the AFM state of the Eu^{2+} ions is suppressed in EuFe_2As_2 in magnetic fields $H \perp c$ exceeding $\mu_0 H \simeq 0.5$ T. For $H \parallel c$, the suppression of the AFM state occurs in fields higher than $\mu_0 H \simeq 1.2$ T since, above this field, the susceptibility for $H \parallel c$ is temperature dependent even at temperature as low as 2 K [see Fig. 3(b)]. Importantly, the magnetic field at which the magnetic moments of the Eu sublattice saturate (i.e., the field at which the FM state is reached) is much higher than the field of suppression of the AFM state. This implies that a FM state appears in a magnetic field higher than the field of suppression of antiferromagnetism and that those two transitions are distinguishable. The peak in the magnetic susceptibility at about 19 K in low fields (see Fig. 2) can be associated with the transition from a PM to a C-AFM state. This peak is shifted to lower temperatures with applied magnetic field above $\mu_0 H \simeq 0.3$ T for $H \perp c$ and above $\mu_0 H \simeq 0.5$ T for $H \parallel c$ [see Figs. 2(b) and 3(b)]. Finally, we may conclude that a field-induced magnetic phase transition from an AFM via a C-AFM configuration to a FM state takes place below 17 K. Such a transition is visible even at the lowest temperature of 2 K reached in our experiment.

The magnetization $M(T)$ in the FM state in the vicinity of the Curie temperature T_C can be described by the power law

$$M(T) = M_0 \left(1 - \frac{T}{T_C}\right)^{\tilde{\beta}}. \quad (2)$$

Here, $\tilde{\beta}$ and M_0 are empirical constants. Analyzing the data at 1.5 T with Eq. (2) yields $T_C = 27.2(1)$ K and $\tilde{\beta} = 0.39(1)$ for both directions of the magnetic field [solid lines in the insets of Figs. 3(a) and 3(b)]. It was found that T_C increases gradually with increasing applied magnetic field for $H \perp c$ and $H \parallel c$. By extrapolating $T_C(H)$ to low fields, the zero-field value of

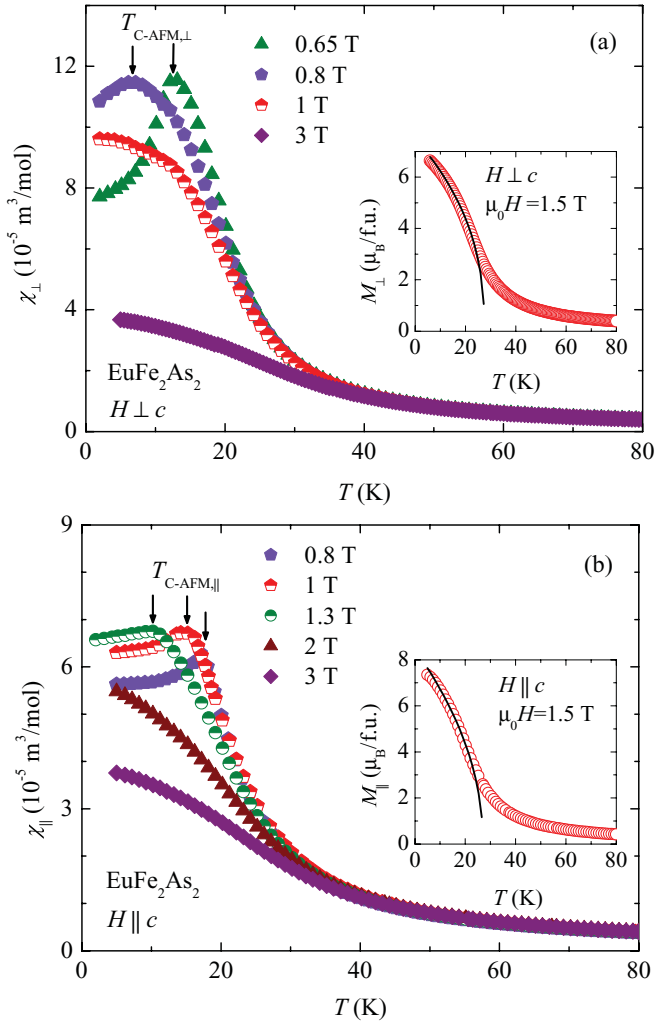


FIG. 3. (Color online) Temperature dependence of the magnetic susceptibility measured at fixed magnetic fields of single-crystal EuFe_2As_2 for $H \perp c$ (a) and $H \parallel c$ (b). The arrows mark the canted antiferromagnetic ordering temperature $T_{\text{C-AFM}}$ of the Eu^{2+} moments in low fields. $T_{\text{C-AFM},\perp}$ and $T_{\text{C-AFM},\parallel}$ refer to the C-AFM ordering temperatures for $H \perp c$ and $H \parallel c$, respectively. The insets illustrate the determination of T_{C} using the power law given in Eq. (2).

T_{C} was found to be $\simeq 19$ K. The present values of $T_{\text{C}}(H)$ are in agreement with those reported by Xiao *et al.*²³

The temperature dependence of the magnetic susceptibility for the Co-doped crystal of $\text{EuFe}_{1.8}\text{Co}_{0.2}\text{As}_2$ in an applied field of $\mu_0 H = 0.01$ T for $H \perp c$ and $H \parallel c$ is presented in Fig. 4. In the inset, the temperature dependence of the difference between the susceptibilities for two field configurations $\chi_{\text{d}} = \chi_{\perp} - \chi_{\parallel}$ is shown. Analyzing the susceptibility data above 30 K with Eq. (1) yields $C = 2108(32) \times 10^{-7} \text{ m}^3 \text{ K/mol}$, $\theta_{\text{CW}} = 21.86(6)$ K for $H \perp c$ and $C = 1915(34) \times 10^{-7} \text{ m}^3 \text{ K/mol}$, $\theta_{\text{CW}} = 20.67(7)$ K for $H \parallel c$. Again, θ_{CW} turns out to be positive. Like in the parent compound, a sharp increase of χ below 30 K is observed, which is attributed to the in-plane FM coupling between the Eu^{2+} moments. Below 17 K, the susceptibility χ_{\perp} starts to decrease with decreasing temperature, indicating the onset of an AFM transition of the Eu^{2+} spins. On the other

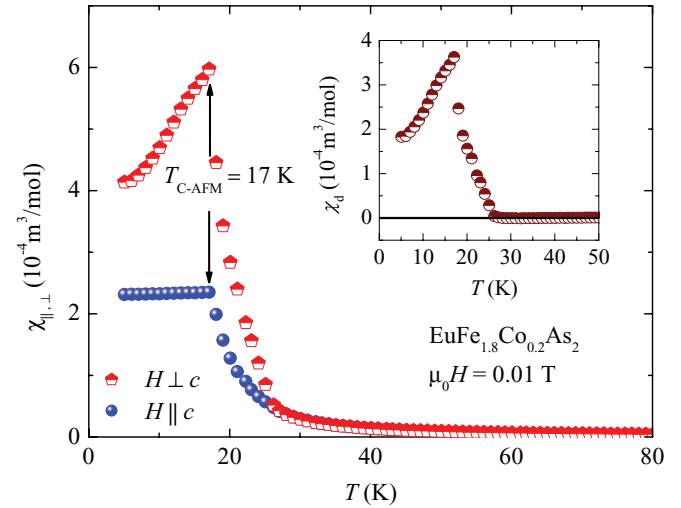


FIG. 4. (Color online) Temperature dependence of the magnetic susceptibility measured in a field of $\mu_0 H = 0.01$ T of single-crystal $\text{EuFe}_{1.8}\text{Co}_{0.2}\text{As}_2$ for $H \perp c$ and $H \parallel c$. The arrows mark the canted antiferromagnetic ordering temperature $T_{\text{C-AFM}} \simeq 17$ K of the Eu^{2+} moments. In the inset, the difference between the susceptibilities for the two different field configurations ($\chi_{\text{d}} = \chi_{\perp} - \chi_{\parallel}$) is plotted as a function of temperature.

hand, χ_{\parallel} remains almost constant below 17 K. This suggests that the Eu^{2+} moments align along the ab plane, similar to undoped EuFe_2As_2 . However, for EuFe_2As_2 , the AFM ordering temperature of the Eu^{2+} spins is about 2 K higher. Below 17 K, χ_{\perp} is significantly larger than χ_{\parallel} , even in magnetic fields as low as $\mu_0 H = 0.01$ T (see Fig. 4). Thus, no crossing between χ_{\perp} and χ_{\parallel} is observed (inset of Fig. 4), in contrast to the parent compound EuFe_2As_2 (see Fig. 2). Furthermore, χ_{\perp} is temperature dependent even at the lowest applied magnetic field. This is inconsistent with an AFM state with an easy c axis. Hence, we suggest that, for all temperatures below 17 K, the ground state of the coupled Eu^{2+} spins in $\text{EuFe}_{1.8}\text{Co}_{0.2}\text{As}_2$ is a C-AFM state with a FM component in the ab plane. This implies that the magnetic configuration of the Eu moments is strongly influenced by the magnetization of the Fe sublattice. This is consistent with previous NMR studies, revealing a strong coupling between the Eu and $\text{Fe}_{2-x}\text{Co}_x\text{As}_2$ layers.³¹

The temperature dependences of χ_{\perp} and χ_{\parallel} at different magnetic fields of single-crystal $\text{EuFe}_{1.8}\text{Co}_{0.2}\text{As}_2$ are shown in Fig. 5. Zero-field cooling (ZFC) and field cooling (FC) susceptibilities $\chi_{\perp}(T)$ measured in an applied field of $\mu_0 H = 0.001$ T are shown in the inset of Fig. 5(a). Below 17 K, the ZFC and FC curves deviate from each other, indicating the presence of a C-AFM state of the Eu^{2+} moments. The data reveal a decrease of the C-AFM ordering temperature $T_{\text{C-AFM}}$ with increasing magnetic field for both field orientations, similar as for the parent compound EuFe_2As_2 . However, the values for $T_{\text{C-AFM}}$ for $\text{EuFe}_{1.8}\text{Co}_{0.2}\text{As}_2$ are substantially smaller than those for EuFe_2As_2 .

2. Field dependence

The susceptibility investigations of the preceding section clearly demonstrate that the system $\text{EuFe}_{2-x}\text{Co}_x\text{As}_2$

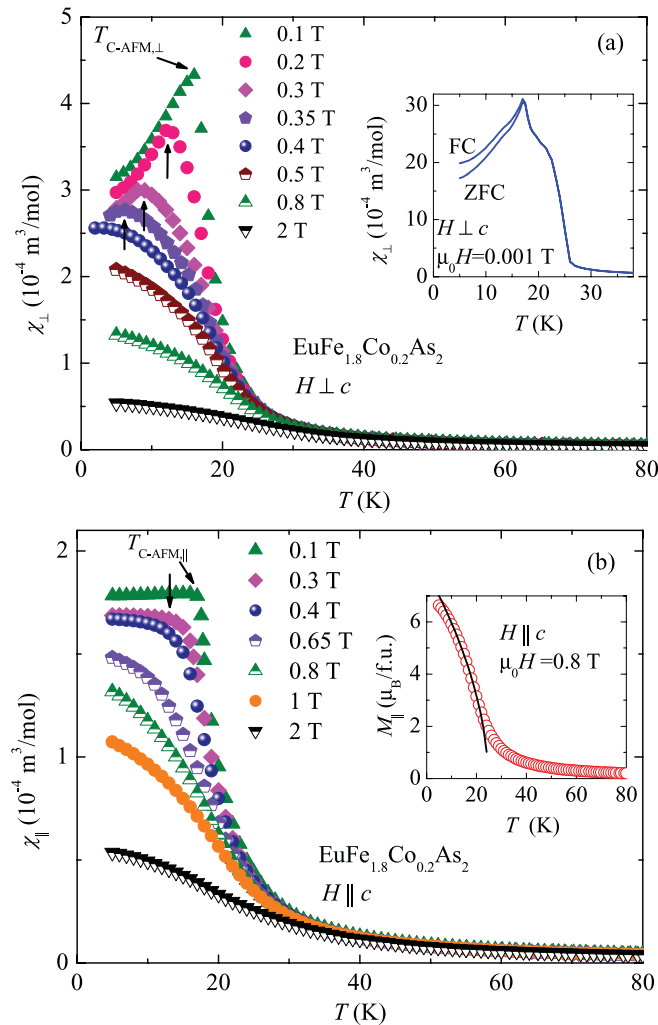


FIG. 5. (Color online) Temperature dependence of the ZFC magnetic susceptibility measured at various fixed magnetic fields of single-crystal $\text{EuFe}_{1.8}\text{Co}_{0.2}\text{As}_2$ for $H \perp c$ (a) and $H \parallel c$ (b). The arrows mark the canted antiferromagnetic ordering temperature $T_{C\text{-AFM}}$ of the Eu^{2+} moments in low magnetic fields. $T_{C\text{-AFM},\perp}$ and $T_{C\text{-AFM},\parallel}$ refer to the C-AFM ordering temperatures for $H \perp c$ and $H \parallel c$, respectively. In the inset of (a), $\chi_{\perp}(T)$ for FC and ZFC in an applied field of $\mu_0 H = 0.001$ T is plotted. The inset of (b) shows the approximation of $M_{\parallel}(T)$ in $\mu_0 H = 0.8$ T by the power law (solid curve) given in Eq. (2).

($x = 0, 0.2$) shows a rich variety of magnetic phases. In order to explore in detail the various magnetic field-induced phases, magnetization experiments were also performed as a function of the applied magnetic field at different temperatures.

The field dependence of the magnetization of single-crystal EuFe_2As_2 at different temperatures for $H \perp c$ is shown in Fig. 6. In the inset, the low-field magnetization M_{\perp} at 5 K is shown. M_{\perp} increases almost linearly with increasing magnetic field H up to $\mu_0 H \simeq 0.45$ T, where a sudden increase of M_{\perp} appears. Then, M_{\perp} further increases with increasing H , and finally saturates for $\mu_0 H \geq 0.8$ T. The value of the saturation magnetization corresponds to an effective magnetic moment of $6.8 \mu_B/f.u.$, which is close to $g\mu_B S = 7 \mu_B/f.u.$ expected for Eu^{2+} moments. This result suggests that there is

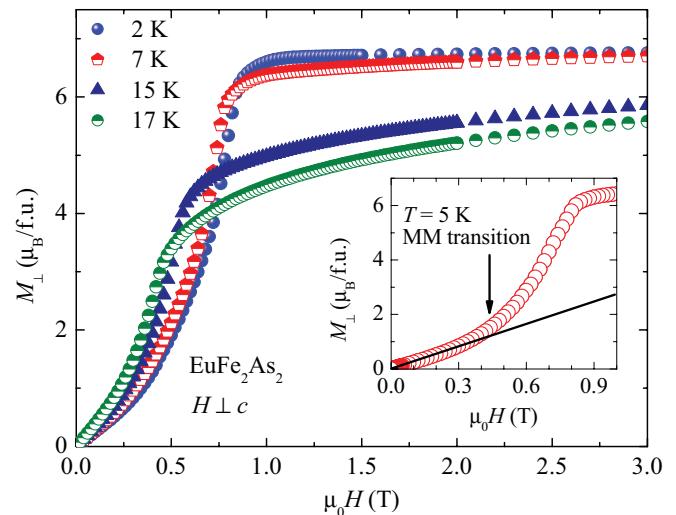


FIG. 6. (Color online) Field dependence of the magnetization at various temperatures of single-crystal EuFe_2As_2 for $H \perp c$. The inset shows the low-field M_{\perp} data at 5 K, illustrating the metamagnetic (MM) transition marked by the arrow.

a metamagnetic^{38,39} (MM) transition at $\mu_0 H_{\text{MM}} \simeq 0.45$ T at 5 K in EuFe_2As_2 , consistent with previous observations.^{20,21} Such a metamagnetic transition is characteristic for A-type antiferromagnetism in layered systems as, e.g., $\text{Na}_{0.85}\text{CoO}_2$ (Ref. 38) and $\text{La}_{2-x}\text{Sr}_{1+x}\text{Mn}_2\text{O}_7$.⁴⁰ Figure 6 shows that the MM transition shifts toward lower fields with increasing temperature. The values of the magnetic field at which the MM transition occurs is in agreement with the results obtained from the susceptibility for the AFM to C-AFM transition. Thus, we propose that the MM transition corresponds to the onset of a spin-flop transition²² from an AFM to a C-AFM state in EuFe_2As_2 . However, no MM transition for $H \perp c$ is detected in $\text{EuFe}_{1.8}\text{Co}_{0.2}\text{As}_2$ [Fig. 7(a)]. Both M_{\perp} and M_{\parallel} first increase almost linearly with increasing H and then saturate at higher fields (Fig. 7). The absence of a MM transition in $\text{EuFe}_{1.8}\text{Co}_{0.2}\text{As}_2$ is consistent with the susceptibility measurements presented above, suggesting that the Eu^{2+} moments exhibit a C-AFM ground state even at very low H . This conclusion is also supported by magnetic hysteresis measurements at 5 K performed in magnetic fields up to 0.5 T. As demonstrated in the inset of Fig. 7(a), the field dependence of M_{\perp} at 5 K shows a well-developed hysteresis for $\text{EuFe}_{1.8}\text{Co}_{0.2}\text{As}_2$, in contrast to the parent compound EuFe_2As_2 where no hysteresis is observed.

Obviously, the presented susceptibility and magnetization measurements reveal a complex and rather sophisticated interplay of magnetic phases in the $\text{EuFe}_{2-x}\text{Co}_x\text{As}_2$ system. Additional information on the complex magnetic phases in $\text{EuFe}_{2-x}\text{Co}_x\text{As}_2$ is obtained from angular-dependent magnetic torque studies presented in the next section.

B. Magnetic torque

In low magnetic fields, the Eu^{2+} magnetic moments prefer to order antiferromagnetically in EuFe_2As_2 . High magnetic fields reorient the magnetic moments, leading to various

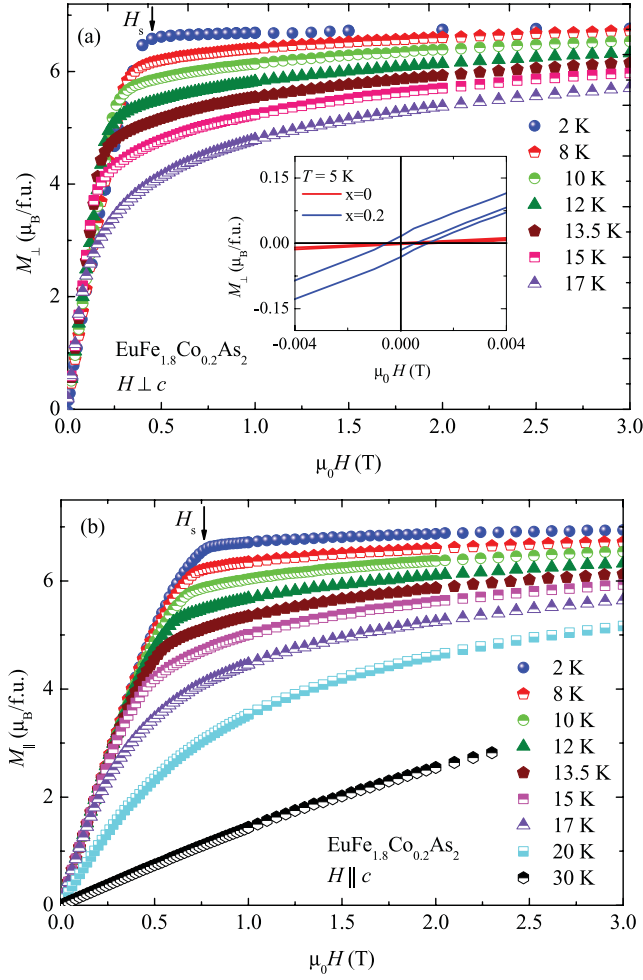


FIG. 7. (Color online) Field dependence of the magnetization at low temperatures of single-crystal $\text{EuFe}_{1.8}\text{Co}_{0.2}\text{As}_2$ for $H \perp c$ (a) and $H \parallel c$ (b). The saturation field H_s at 2 K is marked by arrows. The inset of (a) shows the field dependence of M_{\perp} for EuFe_2As_2 and $\text{EuFe}_{1.8}\text{Co}_{0.2}\text{As}_2$ at 5 K.

magnetic field-induced phases. Magnetic torque allows us to investigate multiple aspects of magnetic order as a function of the magnetic field with respect to the principal axes. Whereas magnetization provides direct information on the magnetic moment oriented along the field, magnetic torque directly probes the anisotropy of the susceptibility in magnetic systems.

The angular dependence of the magnetic torque τ of single-crystal EuFe_2As_2 measured at 13 K in various magnetic fields is presented in Fig. 8(a). In Fig. 8(b), the same data are plotted in terms of $\tau/(\mu_0 H^2)$. The torque data below 0.3 T are of sinusoidal shape, following the simple angular dependence for a uniaxial antiferromagnet⁴¹:

$$\tau(\theta) = -V \frac{(\chi_{\perp} - \chi_{\parallel})}{2} \mu_0 H^2 \sin(2\theta). \quad (3)$$

Here, θ denotes the angle between the field H and the crystallographic c axis, V is the volume of the sample, and χ_{\perp} and χ_{\parallel} are the magnetic susceptibilities for $H \perp c$ and for $H \parallel c$, respectively. Above 0.3 T, the shape of

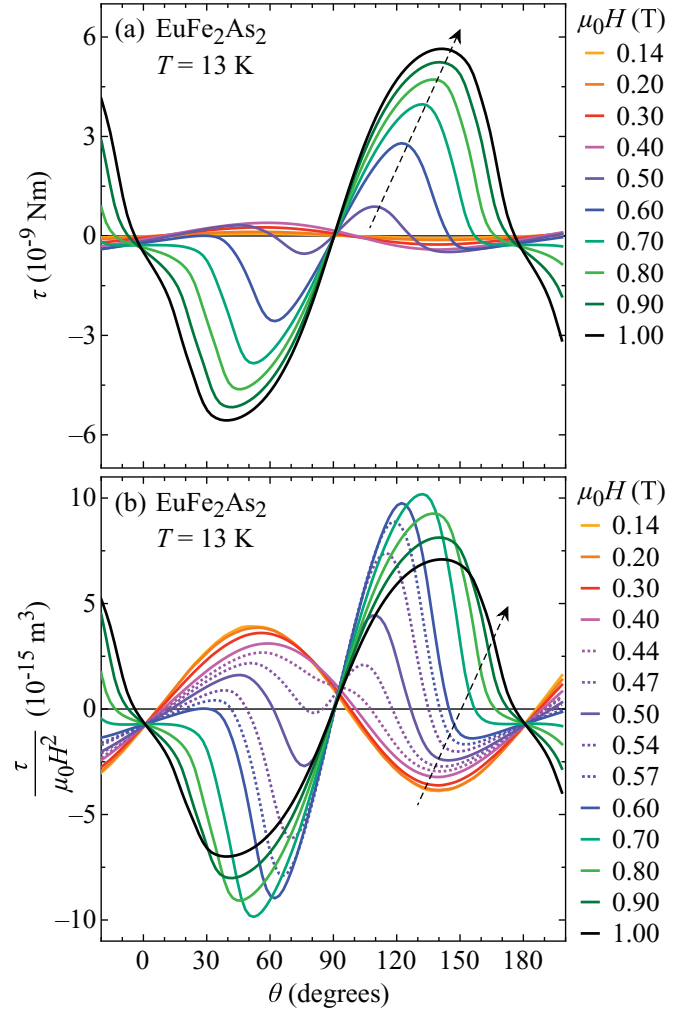


FIG. 8. (Color online) (a) Angular-dependent magnetic torque τ of single-crystal EuFe_2As_2 at 13 K in various magnetic fields. For clarity, not all measured data are shown. (b) Angular dependence of the quantity $\tau/(\mu_0 H^2)$. The dashed arrows denote the direction of increasing magnetic field.

the torque signal changes drastically (see Fig. 8). For $\theta \simeq 90^\circ$ (H almost parallel to the ab plane), an additional torque signal appears, with an opposite sign relative to the AFM torque. Upon increasing the magnetic field, this additional signal rises steeply and leads to a sign change of the torque signal for all angles θ . A similar behavior was observed in RbVBr_3 (Ref. 42) and was interpreted as the appearance of a weak field-induced magnetic moment. This additional contribution to the torque signal observed here is substantially larger than the AFM torque signal. This is consistent with the magnetization data (see Sec. III A), from which the presence of a C-AFM phase was concluded above 0.3 T at 13 K. The sign change of the torque signal is in agreement with the sign change of the quantity $\chi_d = \chi_{\perp} - \chi_{\parallel}$, which was interpreted as a signature of a transition to a C-AFM state of the Eu^{2+} magnetic moments. It was shown previously²⁹ that EuFe_2As_2 exhibits a weak in-plane anisotropy. Since the in-plane anisotropy is much weaker than the out-of-plane anisotropy, this system can be treated approximately

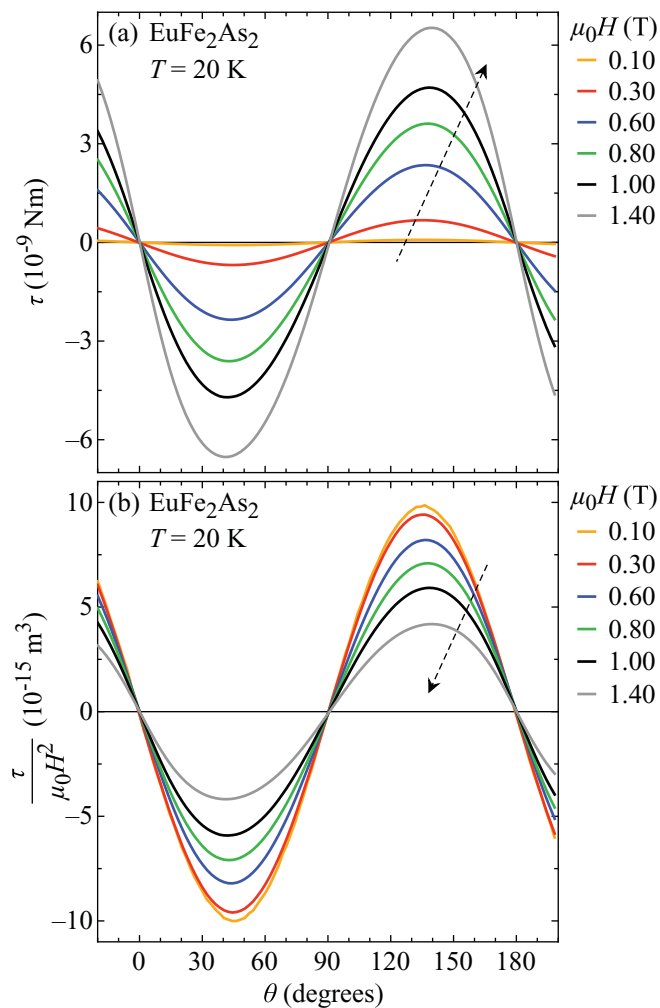


FIG. 9. (Color online) Magnetic torque τ (a) and the quantity $\tau/(\mu_0 H^2)$ (b) as a function of the angle θ of single-crystal EuFe_2As_2 in various magnetic fields at 20 K. The dashed arrows denote the direction of increasing magnetic field.

as a uniaxial anisotropic antiferromagnet. However, even a small in-plane anisotropy may lead to discrepancies between experimental results and theoretical predictions for a uniaxial anisotropic ferromagnet. Particularly, the torque signal of the AFM state shown in Fig. 8(a) is shifted by $\Delta\theta \sim 10^\circ$ with respect to one of the C-AFM state [see Fig. 8(b)]. A similar phase shift $\Delta\theta$ was observed in λ -(BETS) $_2\text{FeCl}_4$ (Ref. 43) and interpreted as a change of the easy axis. However, here the phase shift appears to indicate a crystallographic multidomain state due to a twinning of the crystal in the AFM state.

Figure 9(a) shows the measured magnetic torque for the same EuFe_2As_2 single crystal at 20 K, where, according to the magnetization results, the AFM regime has disappeared. Consistently, no AFM torque signal is observed. Instead, the magnetic torque amplitude increases like H^2 and saturates at higher H . Such a behavior is characteristic for a paramagnet. Consistently, the quantity $\tau/(\mu_0 H^2)$ plotted in Fig. 9(b) decreases with increasing field.

In Fig. 10, the scaled magnetic torque $\tau/(\mu_0 H^2)$ for EuFe_2As_2 and $\text{EuFe}_{1.8}\text{Co}_{0.2}\text{As}_2$ is shown in a color map

for the representative temperatures of 13, 17, and 20 K as a function of angle θ and field H . Note that $\tau/(\mu_0 H^2)$ is scaling according to the magnetic susceptibility. As seen in Fig. 10(a), the low-field regime of undoped EuFe_2As_2 at 13 K is dominated by the AFM state, whereas for higher fields, the C-AFM state appears abruptly along a clearly angular-dependent boundary line (dotted line), demonstrating the anisotropy of this magnetically ordered system. At 17 K [Fig. 10(b)], the AFM phase is not present, consistent with the conclusions from the above susceptibility measurements. At 20 K [Fig. 10(c)], the signal is clearly sinusoidal, consistent with FM behavior. In order to induce a canting of a planar antiferromagnetically ordered subsystem, the in-plane component of the magnetic field H_\perp must overcome the in-plane magnetization \mathcal{M}_\perp in one of the two magnetic sublattices

$$H_\perp \geq A \cdot \mathcal{M}_\perp = A \cdot \sqrt{\mathcal{M}^2 - \mathcal{M}_\parallel^2}. \quad (4)$$

Here, \mathcal{M} is the saturation magnetization of the magnetic sublattice, \mathcal{M}_\parallel its out-of-plane component, and A is a constant. Taking into account

$$H_\perp = H \sin(\theta), \quad (5)$$

$$\mathcal{M}_\parallel = \frac{1}{2} \chi_\parallel H \cos(\theta),$$

where χ_\parallel is the susceptibility of the total Eu^{2+} magnetic sublattice, we obtain for the boundary condition

$$H^2 \sin^2(\theta) = A^2 \left(\mathcal{M}^2 - \frac{1}{4} \chi_\parallel^2 H^2 \cos^2(\theta) \right). \quad (6)$$

Solving this equality for H yields the angle-dependent canting field

$$H_{\text{cant}}(\theta) = \frac{A \cdot \mathcal{M}}{\sqrt{\sin^2(\theta) + \frac{1}{4} \chi_\parallel^2 A^2 \cos^2(\theta)}}. \quad (7)$$

Interestingly, the resulting $H_{\text{cant}}(\theta)$ is analog to the expression for the angular dependence of the upper critical field $H_{c2}(\theta)$ in a type-II superconductor.⁴⁴ Hence, Eq. (7) can be simplified according to

$$H_{\text{cant}}(\theta) = \frac{H_{\text{cant},\perp}}{\sqrt{\sin^2(\theta) + \gamma_{\text{cant}}^{-2} \cos^2(\theta)}}, \quad (8)$$

where $H_{\text{cant},\perp} = H_{\text{cant}}(90^\circ)$ is the in-plane canting field, $\gamma_{\text{cant}} = H_{\text{cant},\parallel}/H_{\text{cant},\perp}$ its anisotropy parameter, and $H_{\text{cant},\parallel} = H_{\text{cant}}(0^\circ)$ the out-of-plane canting field. This shape of the angular dependence of the transition between the AFM and C-AFM phases in the (H, θ) diagram is represented by the dashed line in Fig. 10(a). It describes the experimental torque data rather well, with the parameters $H_{\text{cant},\perp}(13 \text{ K}) \simeq 0.42(2) \text{ T}$ and $\gamma_{\text{cant}} \simeq 2.0(2)$. This yields an estimate of the canting field parallel to the c axis $H_{\text{cant},\parallel}(13 \text{ K}) \simeq 0.84(6) \text{ T}$.

The low-field torque signal of $\text{EuFe}_{1.8}\text{Co}_{0.2}\text{As}_2$ at 20 K [Fig. 10(f)] shows a shape typical for an anisotropic paramagnet. However, the anisotropy of the system is quite quickly suppressed with increasing magnetic field, which may indicate a transformation of the paramagnetic state to a short-range ordered state at relatively low field. It might be caused by large fluctuations of the magnetic moments in the vicinity of the transition from a disordered PM state to an ordered

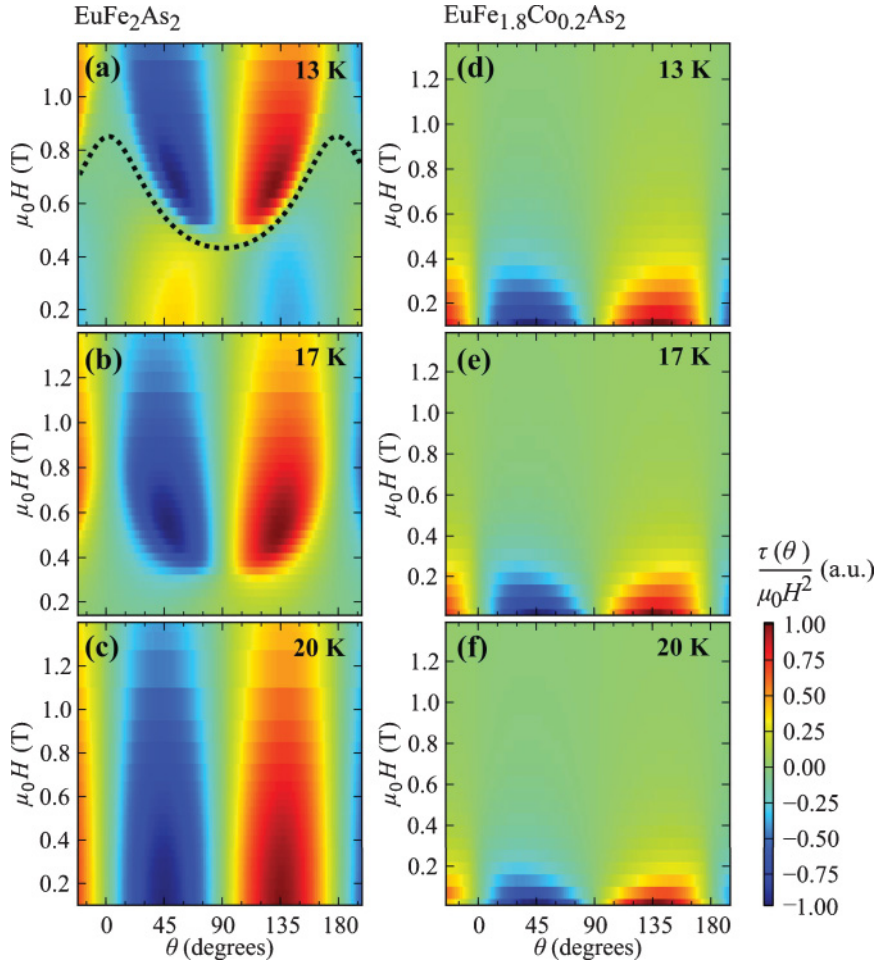


FIG. 10. (Color online) Color map of $\tau/(\mu_0 H^2)$ in arbitrary units (a.u.) for EuFe_2As_2 and $\text{EuFe}_{1.8}\text{Co}_{0.2}\text{As}_2$ as a function of angle θ and field H for $T = 13, 17,$ and 20 K. The dotted line in (a) is calculated according to Eq. (8). Panels (a), (b), and (c) are the data for EuFe_2As_2 at 13, 17, and 20 K, respectively, whereas (d), (e), and (f) are the data for $\text{EuFe}_{1.8}\text{Co}_{0.2}\text{As}_2$ at 13, 17, and 20 K, respectively.

one in $\text{EuFe}_{1.8}\text{Co}_{0.2}\text{As}_2$. Furthermore, at low temperatures, we do not observe any indication of a field-induced transition from the AFM to the C-AFM state [Figs. 10(d) and 10(e)]. Therefore, we conclude that for $\text{EuFe}_{1.8}\text{Co}_{0.2}\text{As}_2$ even at the lowest magnetic field a transition from a PM to a C-AFM state takes place with decreasing temperature, in agreement with the above magnetization data.

IV. DISCUSSION

In Fig. 11, the results of the susceptibility, magnetization, and magnetic torque experiments are summarized. They are discussed in terms of the phase diagram of the Eu^{2+} magnetic sublattice of EuFe_2As_2 and $\text{EuFe}_{1.8}\text{Co}_{0.2}\text{As}_2$ for $H \perp c$ and $H \parallel c$.

A. EuFe_2As_2

For the parent compound EuFe_2As_2 , four different magnetic phases were identified [see Figs. 11(a) and 11(b)]: a paramagnetic (PM), an antiferromagnetic (AFM), a canted antiferromagnetic (C-AFM), and a ferromagnetic (FM) phase. The determination of the corresponding transition temperatures and fields is described in Sec. III. The present experiments suggest a C-AFM order of the Eu^{2+} spins in EuFe_2As_2 in the temperature range between 17 and 19 K, while below 17 K, an AFM structure is proposed. We suggest that, at

low temperatures, the system can be well described with a uniaxial model with easy plane and A-type AFM order. By applying a magnetic field within the AFM phase, a transition from AFM order via a canted configuration to a FM structure is observed. The observed $T_{\text{MM}}(H)$ at which the metamagnetic (MM) transition occurs [open symbols in Fig. 11(a)] is in agreement with the results obtained from the susceptibility for the AFM to C-AFM transition [black filled symbols in Fig. 11(a)]. Thus, we propose that the MM transition corresponds to a spin-flop transition from an AFM to a C-AFM state in EuFe_2As_2 . The critical magnetic field $H_{\text{cr}}(T)$ at which the magnetic moment in the Eu sublattice saturates was determined at different temperatures. The values of H_{cr} extrapolated to zero temperature were found to be $\mu_0 H_{\text{cr},\perp}(0) \simeq 0.85$ T and $\mu_0 H_{\text{cr},\parallel}(0) \simeq 1.5$ T for $H \perp c$ and $H \parallel c$, respectively. By analyzing the shape of the angular dependence of $H_{\text{cr}}(\theta)$ shown in Fig. 10(a), we may conclude that the in-plane component of the magnetic field is responsible for the canting of the spins.

The magnetic ordering of the Eu^{2+} moments at low temperatures is consistent with the magnetic structure established by neutron diffraction at 2.5 K.⁵ Note that, in previous reports,^{20,21} a possible C-AFM state in the temperature range $17 \text{ K} \leq T \leq 19 \text{ K}$ was not discussed. To our knowledge, no neutron data for the magnetic configuration of the Eu sublattice in this temperature range are available.

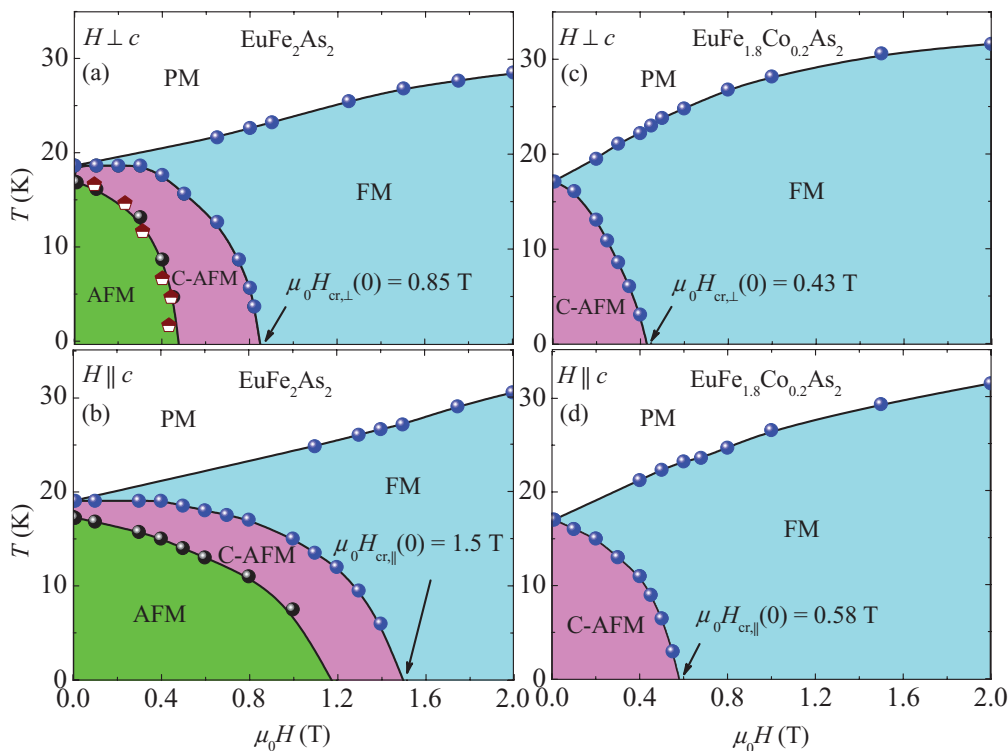


FIG. 11. (Color online) Magnetic phase diagrams of single-crystal EuFe_2As_2 [(a) and (b)] and single-crystal $\text{EuFe}_{1.8}\text{Co}_{0.2}\text{As}_2$ [(c) and (d)] for $H \perp c$ and for $H \parallel c$. The various phases in the phase diagrams are denoted as follows: paramagnetic (PM), antiferromagnetic (AFM), canted antiferromagnetic (C-AFM), and ferromagnetic (FM). The filled and open symbols are from the susceptibility and field-dependent magnetization measurements, respectively. The solid lines are guides to the eyes.

B. $\text{EuFe}_{1.8}\text{Co}_{0.2}\text{As}_2$

The corresponding magnetic phase diagrams for Co-doped $\text{EuFe}_{1.8}\text{Co}_{0.2}\text{As}_2$ are shown in Figs. 11(c) and 11(d). The magnetic ordering temperature of $\simeq 17$ K is only about 2 K lower as compared to the parent compound. However, in the Co-doped $\text{EuFe}_{1.8}\text{Co}_{0.2}\text{As}_2$, no signatures of a low-field and low-temperature AFM state of the Eu^{2+} moments were found. Only a C-AFM phase (with a FM component in the ab plane) is present at low fields and low temperatures. The ordering temperature $T_{\text{C-AFM}}$ decreases with increasing magnetic field, similar to the parent compound [see Figs. 11(a) and 11(b)]. The critical magnetic field H_{cr} at which the Eu magnetic ordering is saturated was determined for different temperatures, and the extrapolated zero-temperature values were found to be $\mu_0 H_{\text{cr},\perp}(0) \simeq 0.43$ T and $\mu_0 H_{\text{cr},\parallel}(0) \simeq 0.58$ T for $H \perp c$ and $H \parallel c$, respectively. These values of $\mu_0 H_{\text{cr}}$ are much smaller than those obtained for the parent compound. Moreover, the magnetic anisotropy $\gamma_{\text{cr}} = H_{\text{cr},\parallel}(0)/H_{\text{cr},\perp}(0) \simeq 1.35$ of Co-doped $\text{EuFe}_{1.8}\text{Co}_{0.2}\text{As}_2$ is also smaller than $\gamma_{\text{cr}} \simeq 1.76$ of the parent compound.

It was concluded from different experiments^{21,27,29–31} that there is a strong coupling between the localized Eu^{2+} spins and the conduction electrons of the two-dimensional (2D) Fe_2As_2 layers. Recently, direct experimental evidence for a strong interlayer coupling was obtained by means of ^{75}As NMR,³¹ revealing a magnetic exchange interaction between the localized Eu 4*f* moments, which is mediated by the itinerant Fe 3*d* electrons. However, the direct interaction of the Eu moments and the magnetic moments in Fe sublattice

can not be neglected. Only a combination of both interactions can further elucidate the C-AFM ground state observed in the parent compound EuFe_2As_2 as well as in the Co-doped system $\text{EuFe}_{1.8}\text{Co}_{0.2}\text{As}_2$ (see Fig. 11).

Note that the present results for $\text{EuFe}_{1.8}\text{Co}_{0.2}\text{As}_2$, exhibiting a SDW ground state below 60 K,³⁰ reveal a C-AFM structure of the Eu spins with a FM component in the ab plane. This finding confirms previous assumptions that, for materials in which the Fe ions are in the SDW ground state (such as EuFe_2As_2), the direction of the Eu magnetic moments is in the ab plane.^{5,32} On the other hand, in the case of nonmagnetic Fe ground states, like in superconducting $\text{EuFe}_{2-x}\text{Co}_x\text{As}_2$ compounds, where the SDW magnetic state is totally suppressed, the direction of the Eu magnetic moments is parallel to the c axis.^{33–36}

V. CONCLUSIONS

The magnetic properties of single crystals of EuFe_2As_2 and $\text{EuFe}_{1.8}\text{Co}_{0.2}\text{As}_2$ were studied by means of susceptibility, magnetization, and magnetic torque investigations. The susceptibility and magnetization experiments performed for various temperatures and magnetic fields along the crystallographic axes provided information on the magnetic structure of the studied crystals. In addition, the evolution of the magnetic structure as a function of the tilting angle of the field and the crystallographic axes is studied by magnetic torque experiments. The phase diagrams for the ordering of the Eu^{2+} magnetic sublattice with respect to temperature, magnetic field, and the angle between the magnetic field

and the crystallographic c axis in $\text{EuFe}_{2-x}\text{Co}_x\text{As}_2$ are determined and discussed. The present investigations reveal a complex and sophisticated interplay of magnetic phases in $\text{EuFe}_{2-x}\text{Co}_x\text{As}_2$. The magnetic ordering temperature of the Eu^{2+} moments remains nearly unchanged upon Co doping. However, unlike the parent compound, in which the Eu^{2+} moments order antiferromagnetically at low temperatures, the Co-doped system $\text{EuFe}_{1.8}\text{Co}_{0.2}\text{As}_2$ exhibits a C-AFM state with a FM component in the ab plane. The magnetic anisotropy γ_{cr} becomes smaller as a result of Co doping. This implies that the magnetic configuration of the Eu moments is strongly influenced by the magnetic moments of the Fe sublattice, where superconductivity takes place for a certain range of

Co doping. A detailed knowledge of the interplay between the Eu^{2+} moments and magnetism of the Fe sublattice is important to understand the role of magnetism of the localized Eu^{2+} moments for the occurrence of superconductivity in $\text{EuFe}_{2-x}\text{Co}_x\text{As}_2$.

ACKNOWLEDGMENT

This work was supported by the Swiss National Science Foundation, the SCOPES Grant No. IZ73Z0_128242, the NCCR Project MaNEP, the EU Project CoMePhS, and the Georgian National Science Foundation Grant No. GNSF/ST08/4-416.

*zurabgug@physik.uzh.ch

†Current address: Institute of Low Temperature and Structure Research, Polish Academy of Sciences, 50-422 Wrocław, Poland.

¹Y. Kamihara, T. Watanabe, M. Hirano, and H. Hosono, *J. Am. Chem. Soc.* **130**, 3296 (2008).

²X. H. Chen, T. Wu, G. Wu, R. H. Liu, H. Chen, and D. F. Fang, *Nature (London)* **453**, 761 (2008).

³M. Rotter, M. Tegel, and D. Johrendt, *Phys. Rev. Lett.* **101**, 107006 (2008).

⁴F.-C. Hsu, J.-Y. Luo, K.-W. Yeh, T.-K. Chen, T.-W. Huang, P. M. Wu, Y.-C. Lee, Y.-L. Huang, Y.-Y. Chu, D.-C. Yan, and M.-K. Wu, *Proc. Natl. Acad. Sci. USA* **105**, 14262 (2008).

⁵Y. Xiao, Y. Su, M. Meven, R. Mittal, C. M. N. Kumar, T. Chatterji, S. Price, J. Persson, N. Kumar, S. K. Dhar, A. Thamizhavel, and Th. Brueckel, *Phys. Rev. B* **80**, 174424 (2009).

⁶M. S. Torikachvili, S. L. Bud'ko, N. Ni, and P. C. Canfield, *Phys. Rev. Lett.* **101**, 057006 (2008).

⁷Liling Sun, Jing Guo, Genfu Chen, Xianhui Chen, Xiaoli Dong, Wei Lu, Chao Zhang, Zheng Jiang, Yang Zou, Suo Zhang, Yuying Huang, Qi Wu, Xi Dai, Yuanchun Li, Jing Liu, and Zhongxian Zhao, *Phys. Rev. B* **82**, 134509 (2010).

⁸H. Lee, E. Park, T. Park, V. A. Sidorov, F. Ronning, E. D. Bauer, and J. D. Thompson, *Phys. Rev. B* **80**, 024519 (2009).

⁹P. L. Alireza, Y. T. C. Ko, J. Gillett, C. M. Petrone, J. M. Cole, G. G. Lonzarich, and S. E. Sebastian, *J. Phys. Condens. Matter* **21**, 012208 (2009).

¹⁰K. Igawa, H. Okada, H. Takahashi, S. Matsuishi, Y. Kamihara, M. Hirano, H. Hosono, K. Matsubayashi, and Y. Uwatoko, *J. Phys. Soc. Jpn.* **78**, 025001 (2009).

¹¹H. Fukazawa, N. Takeshita, T. Yamazaki, K. Kondo, K. Hirayama, Y. Kohori, K. Miyazawa, H. Kito, H. Eisaki, and A. Iyo, *J. Phys. Soc. Jpn.* **77**, 105004 (2008).

¹²W. J. Duncan, O. P. Welzel, C. Harrison, X. F. Wang, X. H. Chen, F. M. Grosche, and P. G. Niklowitz, *J. Phys. Condens. Matter* **22**, 052201 (2010).

¹³A. Mani, N. Ghosh, S. Paulraj, A. Bharathi, and C. S. Sundar, *Europhys. Lett.* **87**, 17004 (2009).

¹⁴T. Terashima, M. Kimata, H. Satsukawa, A. Harada, K. Hazama, S. Uji, H. S. Suzuki, T. Matsumoto, and K. Murata, *J. Phys. Soc. Jpn.* **78**, 083701 (2009).

¹⁵C. F. Miclea, M. Nicklas, H. S. Jeevan, D. Kasinathan, Z. Hossain, H. Rosner, P. Gegenwart, C. Geibel, and F. Steglich, *Phys. Rev. B* **79**, 212509 (2009).

¹⁶Z. A. Ren, W. Lu, J. Yang, W. Yi, X. L. Shen, Z. C. Li, G. C. Che, X. L. Dong, L. L. Sun, F. Zhou, and Z. X. Zhao, *Chin. Phys. Lett.* **25**, 2215 (2008).

¹⁷S. Matsuishi, Y. Inoue, T. Nomura, M. Hirano, and H. Hosono, *J. Phys. Soc. Jpn.* **77**, 113709 (2008).

¹⁸J. Zhao, Q. Huang, C. de la Cruz, S. Li, J. W. Lynn, Y. Chen, M. A. Green, G. F. Chen, G. Li, Z. Li, J. L. Luo, N. L. Wang, and P. Dai, *Nat. Mater.* **7**, 953 (2008).

¹⁹H. Raffius, E. Mörsen, B. D. Mosel, W. Müller-Warmuth, W. Jeitschko, L. Terbüchte, and T. Vomhof, *J. Phys. Chem. Solids* **54**, 135 (1993).

²⁰Z. Ren, Z. W. Zhu, S. Jiang, X. F. Xu, Q. Tao, C. Wang, C. M. Feng, G. H. Cao, and Z. A. Xu, *Phys. Rev. B* **78**, 052501 (2008).

²¹S. Jiang, Y. K. Luo, Z. Ren, Z. W. Zhu, C. Wang, X. F. Xu, Q. Tao, G. H. Cao, and Z. A. Xu, *New J. Phys.* **11**, 025007 (2009).

²²S. Blundell, *Magnetism in Condensed Matter* (Oxford University Press, New York, 2006).

²³Y. Xiao, Y. Su, W. Schmidt, K. Schmalzl, C. M. N. Kumar, S. Price, T. Chatterji, R. Mittal, L. J. Chang, S. Nandi, N. Kumar, S. K. Dhar, A. Thamizhavel, and Th. Brueckel, *Phys. Rev. B* **81**, 220406 (2010).

²⁴Shuai Jiang, Hui Xing, Guofang Xuan, Zhi Ren, Cao Wang, Zhu-an Xu, and Guanghan Cao, *Phys. Rev. B* **80**, 184514 (2009).

²⁵Y. He, T. Wu, G. Wu, Q. J. Zheng, Y. Z. Liu, H. Chen, J. J. Ying, R. H. Liu, X. F. Wang, Y. L. Xie, Y. J. Yan, J. K. Dong, S. Y. Li, and X. H. Chen, *J. Phys. Condens. Matter* **22**, 235701 (2010).

²⁶H. S. Jeevan, Deepa Kasinathan, H. Rosner, and P. Gegenwart, *Phys. Rev. B* **83**, 054511 (2011).

²⁷Zhi Ren, Xiao Lin, Qian Tao, Shuai Jiang, Zengwei Zhu, Cao Wang, Guanghan Cao, and Zhu'an Xu, *Phys. Rev. B* **79**, 094426 (2009).

²⁸L. J. Li, Y. K. Luo, Q. B. Wang, H. Chen, Z. Ren, Q. Tao, Y. K. Li, X. Lin, M. He, Z. W. Zhu, G. H. Cao, and Z. A. Xu, *New J. Phys.* **11**, 025008 (2009).

²⁹E. Dengler, J. Deisenhofer, H. A. Krug von Nidda, Seunghyun Khim, J. S. Kim, Kee Hoon Kim, F. Casper, C. Felser, and A. Loidl, *Phys. Rev. B* **81**, 024406 (2010).

³⁰J. J. Ying, T. Wu, Q. J. Zheng, Y. He, G. Wu, Q. J. Li, Y. J. Yan, Y. L. Xie, R. H. Liu, X. F. Wang, and X. H. Chen, *Phys. Rev. B* **81**, 052503 (2010).

³¹Z. Guguchia, J. Roos, A. Shengelaya, S. Katrych, Z. Bukowski, S. Weyeneth, F. Murányi, S. Strässle, A. Maisuradze, J. Karpinski, and H. Keller, *Phys. Rev. B* **83**, 144516 (2011).

³²I. Nowik and I. Felner, *Hyperfine Interact.* **28**, 959 (1986).

³³I. Nowik and I. Felner, *Physica C* **469**, 485 (2009).

- ³⁴C. Feng, Z. Ren, S. Xu, S. Jiang, Z. Xu, G. Cao, I. Nowik, I. Felner, K. Matsubayashi, and Y. Uwatoko, *Phys. Rev. B* **82**, 094426 (2010).
- ³⁵I. Nowik, I. Felner, Z. Ren, G. H. Cao, and Z. A. Xu, *J. Phys. Condens. Matter* **23**, 065701 (2011).
- ³⁶I. Nowik, I. Felner, Z. Ren, G. H. Cao, and Z. A. Xu, *New J. Phys.* **13**, 023033 (2011).
- ³⁷S. Kohout, J. Roos, and H. Keller, *Rev. Sci. Instrum.* **78**, 013903 (2007).
- ³⁸J. L. Luo, N. L. Wang, G. T. Liu, D. Wu, X. N. Jing, F. Hu, and T. Xiang, *Phys. Rev. Lett.* **93**, 187203 (2004).
- ³⁹R. S. Perry, L. M. Galvin, S. A. Grigera, L. Capogna, A. J. Schofield, A. P. Mackenzie, M. Chiao, S. R. Julian, S. I. Ikeda, S. Nakatsuji, Y. Maeno, and C. Pfleiderer, *Phys. Rev. Lett.* **86**, 2661 (2001).
- ⁴⁰T. Kimura and Y. Tokura, *Ann. Rev. Mater. Sci.* **30**, 451 (2000).
- ⁴¹S. Weyeneth, P. J. W. Moll, R. Puzniak, K. Ninios, F. F. Balakirev, R. D. McDonald, H. B. Chan, N. D. Zhigadlo, S. Katrych, Z. Bukowski, J. Karpinski, H. Keller, B. Batlogg, and L. Balicas, *Phys. Rev. B* **83**, 134503 (2011).
- ⁴²H. Tanaka, T. Kato, K. Iio, and K. Nagata, *J. Phys. Soc. Jpn.* **61**, 3292 (1992).
- ⁴³T. Sasaki, H. Uozaki, S. Endo, and N. Toyota, *Synth. Metals* **120**, 759 (2001).
- ⁴⁴G. Blatter, M. V. Feigel'man, V. B. Geshkenbein, A. I. Larkin, and V. M. Vinokur, *Rev. Mod. Phys.* **66**, 1125 (1994).